Clinical and Experimental Obstetrics & Gynecology

Clin. Exp. Obstet. Gynecol. **2026**; 53(9): 52944
https://doi.org/10.31083/CEOG52944

Original Research

LIMCH1 is Downregulated and Associated With Poor Prognosis, and Suppresses Tumor Cell Proliferation and Invasion in Ovarian Cancer

Pengfeng Zhu[1,2,†], Xiang Fan[2,†], Yifei Wang[2], Jia Yang[2], Yunlang Cai[3,*]

[1]School of Medicine, Southeast University, 210009 Nanjing, Jiangsu, China
[2]Department of Gynecology, Changzhou Maternal and Child Health Care Hospital, Changzhou Medical Center, Nanjing Medical University, 213000 Changzhou, Jiangsu, China
[3]Department of Obstetrics and Gynecology, Zhongda Hospital, School of Medicine, Southeast University, 210009 Nanjing, Jiangsu, China
*Correspondence: caiyl2021@163.com (Yunlang Cai)
[†]These authors contributed equally.

Academic Editor: Michael H. Dahan
Submitted: 15 April 2026 Revised: 7 July 2026 Accepted: 21 July 2026 Published: 15 September 2026

Abstract

Background: LIM and calponin homology domain-containing protein 1 (LIMCH1) regulates myosin stress fiber assembly and cell motility and is involved in carcinogenesis. However, its role in ovarian cancer remains poorly characterized. In this study, LIMCH1 was identified as a candidate tumor suppressor gene through analysis of Gene Expression Omnibus (GEO) datasets, and its clinical relevance and regulatory function in ovarian cancer were investigated. **Methods:** The GSE102094, GSE160626, and GSE190688 datasets were used to identify differentially expressed genes (DEGs) between ovarian cancer tissues and control tissues, whereas the GSE102094 and GSE160626 datasets were used to identify DEGs between platinum-resistant and platinum-sensitive ovarian cancer tissues. Gene Expression Profiling Interactive Analysis (GEPIA) was used to evaluate the clinical relevance of LIMCH1 in ovarian cancer, and the findings were further validated by immunohistochemical analysis of 70 ovarian cancer tissues and 10 control tissues. Functional validation of LIMCH1 was performed by transfecting SKOV3 and CAOV-3 cells with LIMCH1 overexpression plasmids or LIMCH1-specific siRNA. A xenograft model was established by injecting SKOV3 cells transduced with either LIMCH1-overexpressing lentivirus or NC lentivirus. **Results:** A total of 177 DEGs were identified by intersecting ovarian cancer-associated DEGs with platinum resistance-associated DEGs, which were mainly enriched in pathways related to cell cycle regulation, cell junctions, and carcinogenesis. Among these candidates, LIMCH1 was selected for further exploration. Analysis of the GEPIA database demonstrated that LIMCH1 expression was significantly reduced in ovarian cancer tissues, and markedly low LIMCH1 expression was associated with poor overall survival in patients with ovarian cancer. Immunohistochemical analysis further confirmed the downregulation of LIMCH1 expression in ovarian cancer tissues. Moreover, LIMCH1 expression showed good diagnostic performance for distinguishing ovarian cancer from the control tissues, with an area under the receiver operating characteristic curve (AUC) of 0.794. Furthermore, LIMCH1 expression was negatively correlated with tumor stage and pathological grade. *In vitro* experiments discovered that LIMCH1 suppressed SKOV3 and CAOV-3 cell proliferation and invasion, while promoting apoptosis and increasing carboplatin sensitivity. *In vivo* experiments further showed that LIMCH1 inhibited tumor progression. **Conclusions:** These findings suggest that LIMCH1 may function as a novel tumor suppressor involved in the pathogenesis of ovarian cancer.

Keywords: ovarian cancer; GEO datasets; LIMCH1; clinical relevance; regulatory function

1. Introduction

Ovarian cancer is among the most prevalent gynecological malignancies, with 324,000 new cases and 207,000 cancer-related deaths per year globally, and 61,000 new cases and 33,000 cancer-related deaths per year in China [1,2]. Surgical excision remains the cornerstone of ovarian cancer management, also enabling accurate staging and risk stratification to guide subsequent therapy [3,4,5]. Following surgery, platinum-based adjuvant chemotherapy remains the standard of care for eliminating residual tumor cells and reducing the risk of recurrence [6,7]. This treatment strategy has significantly improved patient outcomes and survival.

Although a majority of ovarian cancer patients benefit from platinum-based chemotherapy, approximately 20%–30% exhibit poor responses to first-line treatment or experience early relapse [8]. The emergence of platinum-resistant disease is a major clinical challenge in ovarian cancer, underscoring the need for alternative therapeutic strategies, including targeted therapies [9,10]. Clinically, Poly ADP-ribose polymerase (PARP) inhibitors and vascular endothelial growth factor (VEGF) inhibitors are commonly administered, with or without chemotherapy, thereby prolonging the survival [11,12]. The former inhibits PARP enzymes involved in DNA repair, thereby inducing death of tumor cells with homologous recombination defects, while the latter inhibits tumor angiogenesis and enhances the cytotoxic effect of chemotherapy [11,12]. In addition to these, un-

derlying molecular mechanisms and corresponding potential targets are being explored, particularly with advances in high-throughput technologies [13,14,15,16].

This study aimed to identify candidate genes implicated in ovarian cancer development and platinum resistance by analyzing Gene Expression Omnibus (GEO) datasets. Among the identified candidates, LIM and calponin homology domain-containing protein 1 (LIMCH1) was selected for further investigation, and its function was subsequently validated in ovarian cancer clinical samples and cells.

2. Materials and Methods

2.1 GEO Datasets Collection and Bioinformatic Analysis

Three ovarian cancer transcription datasets (GSE102094, GSE160626, and GSE190688) were obtained from the GEO database (https://www.ncbi.nlm.nih.gov/geo/). GSE102094 (GSE102073 subseries) contained RNA sequencing data from 85 ovarian cancer tissues, 3 normal fallopian tube tissues, 3 normal peritoneal tissues, and 4 normal ovary tissues. 70 out of 85 ovarian cancer cases received platinum-based therapy, then classified as platinum-sensitive (n = 59) and platinum-resistant (n = 11). GSE160626 included RNA sequencing data from 18 ovarian cancer tissues and 7 normal ovarian tissues. All 18 ovarian cancer cases received platinum-based therapy and were classified as platinum-sensitive (n = 10) and platinum-resistant (n = 8). GSE190688 comprised RNA sequencing data from 6 ovarian cancer tissues and 5 normal fallopian tube tissues.

Bioinformatic analysis was performed using R software (version 4.3.0; R Core Team, Vienna, Austria). Differential expression analysis was conducted using the DESeq2 package, and results were visualized using volcano plots. For comparison between ovarian cancer (OC) and control (Control) tissues, genes with an adjusted $p < 0.05$ and $|\log_2(\text{fold change})| > 1$ were defined as differentially expressed genes (DEGs). For comparison of platinum-resistant (Res) versus platinum-sensitive (Sen) samples, owing to the limited number of DEGs identified using the threshold of fold change at 2, the threshold at 1.5 was applied; therefore, DEGs were identified using a threshold of an adjusted $p < 0.05$ and $|\log_2(\text{fold change})| > 0.585$.

The genes commonly dysregulated across datasets were identified by intersecting DEGs from the OC versus Control comparisons. The results were subsequently visualized using a Venn diagram. Additionally, an intersection analysis was performed between the common OC versus Control DEGs and the union of DEGs derived from the Res vs. Sen comparisons, with results presented as a Venn diagram. Gene Ontology (GO) and Kyoto Encyclopedia of Genes and Genomes (KEGG) pathway enrichment analyses were performed using the clusterProfiler package. The results of these enrichment analyses were visualized using ggplot2. Considering the biological heterogeneity of platinum resistance across different cohorts, genes overlapping with the ovarian cancer-related DEGs and at least one platinum-resistance dataset were retained for subsequent analyses, rather than restricting the selection to the three-way intersection only.

2.2 Gene Expression Profiling Interactive Analysis (GEPIA)

The GEPIA public database [17] was used to analyze the expression levels of LIMCH1 and snail family transcriptional repressor 3 (SNAI3) in ovarian cancer, and to assess their correlations with tumor stage and survival, using the Box Plot, Stage Plot, and Survival Plot modules.

2.3 Sample Collection and Immunohistochemistry (IHC)

All protocols received approval from the Medical Ethics Committee of Changzhou Maternal and Child Health Care Hospital (approval No. 2023 [156], approval date: October 11, 2023), with written informed consent obtained from patients or their families. The study was conducted in accordance with the Declaration of Helsinki. Seventy tumor tissues and 10 control tissues were included in this study. The cancer tissues were obtained from ovarian cancer patients who underwent tumor resection. The control tissues were collected from patients who underwent oophorectomy for benign gynecological conditions. All human samples were collected from February 2019 to September 2023. LIMCH1 expression was detected by IHC in 70 tumor tissues and 10 control tissues, and SNAI3 expression was detected by IHC in 10 tumor and 10 control tissues, respectively.

After resection, the tissues were fixed in 10% formalin for 24 hours before embedding in paraffin. Sections of 4 μm thickness were prepared, deparaffinized using Deparaffinization Buffer (Cat No. G1128, Servicebio, Wuhan, Hubei, China), and rehydrated through graded ethanol concentrations (Cat No. 10009161, Sinopharm, Shanghai, China). Endogenous peroxidase was removed by treating the sections with 3% H_2O_2. Antigen retrieval was performed by microwave heating in citric acid antigen retrieval buffer (pH 6.0). Subsequently, the sections were incubated with LIMCH1 antibody (1:150, Cat No. DF14832, Affinity, Liyang, Jiangsu, China) or SNAI3 antibody (1:250, Cat No. 21350-1-AP, Proteintech, Wuhan, Hubei, China) at 4 ℃ overnight, followed by treatment with HRP-conjugated Secondary Antibody (dilution 1:1000, Cat No. GB23303, Servicebio, Wuhan, Hubei, China) at 37 ℃ for 1 h. The sections were then stained with DAB Solution (Cat No. G1212, Servicebio, Wuhan, Hubei, China) for 5 minutes and counterstained with Hematoxylin (Cat No. 1004, Servicebio, Wuhan, Hubei, China), dehydrated, and mounted. Images were captured using an inverted microscope (AE31, Motic, Xiamen, Fujian, China).

The IHC score was calculated by multiplying the staining intensity by the staining density (resulting in a 0–12

points). The staining intensity was scored 0–3: 0, no staining; 1, weak staining (light yellow); 2, moderate staining (yellowish-brown); 3, strong staining (brown). The staining density was scored on a scale of 0–4 according to the percentage of positive cells as follows: 0 (0%), 1 (1–25%), 2 (26–50%), 3 (51–75%), and 4 (76–100%).

2.4 Cell Culture and Transfection

Human ovarian cancer cell line SKOV3 (Cat No. iCell-h195, Cellverse, Shanghai, China) and CAOV-3 (Cat No. CL-0055, Procell, Wuhan, Hubei, China) was cultured in McCoy's 5A Medium (Cat No. G4540, Servicebio, Wuhan, Hubei, China) and Dulbecco's Modified Eagle Medium (Cat No. G4581, Servicebio, Wuhan, Hubei, China), respectively. Fetal Bovine Serum (FBS, Cat No. 164210, Procell, Wuhan, Hubei, China) was supplemented to a final concentration of 10%. A humid condition with 5% CO_2 and 37 ℃ was provided. All cell lines tested negative for mycoplasma contamination, and were authenticated by short tandem repeat (STR) analysis, which was performed by Cellverse (Wuhan, Hubei, China) or Procell (Wuhan, Hubei, China). No misidentification or cross-contamination was identified according to the ExPASy Cellosaurus database. The SKOV3 and CAOV-3 cells were transfected with a LIMCH1 overexpression plasmid using the GV661 vector (Genechem, Shanghai, China) or LIMCH1 small interfering RNA (siRNA, Genepharma, Shanghai, China) using GP-transfect-mate (Cat No. G04009, Genepharma, Shanghai, China). The negative control (NC) plasmid and siRNA were also transfected into cells. The cells cultured under normal conditions served as a control. The siRNA sequences were listed: LIMCH1 siRNA (sense, 5'-CAGGACUGGACAAUAUUAUTT-3; antisense, AUAAUAUUGUCCAGUCCUGTT) and negative control siRNA (sense, UUCUCCGAACGUGUCACGUTT; antisense, ACGUGACACGUUCGGAGAATT).

2.5 Immunoblotting

The SKOV3 and CAOV-3 cells were lysed in RIPA Buffer (Cat No. G2002, Servicebio, Wuhan, Hubei, China) at 48 h post-transfection. The protein concentration of the lysate was measured using a BCA Kit (Cat No. G2026, Servicebio, Wuhan, Hubei, China). A 20 µg aliquot of the lysate was denatured and loaded onto a Precast Gel (Willget, Shanghai, China), and the protein was transferred onto a Nitrocellulose Membrane (Cat No. YA1711, Solarbio, Beijing, China). The membrane was blocked with 5% BSA (Cat No. GC305010, Servicebio, Wuhan, Hubei, China) at 37 ℃ for 1 h. Subsequently, the membrane was incubated with LIMCH1 antibody (1:2000) and GAPDH antibody (1:10,000, Cat No. AF7021, Affinity, Liyang, Jiangsu, China) overnight at 4 ℃. After antibody incubation, the membrane was rinsed and covered with the HRP-linked secondary antibody (1:20,000). Finally, the protein bands on the membrane were visualized using the ECL Kit (Cat No. G2161, Servicebio, Wuhan, Hubei, China).

2.6 Cell Proliferation, Apoptosis, and Transwell Assay

For cell proliferation, cells were seeded into 96-well plates at 48 h post-transfection. To prepare a working solution, 10 µL of CCK-8 reagent (Cat No. G1613, Servicebio, Wuhan, Hubei, China) was combined with 100 µL of McCoy's 5A medium. At each designated time point post-seeding, the working solution was added to the wells. The plates were then incubated at 37 ℃ for an additional 2 h. Subsequently, the optical density (OD) was measured at 450 nm using a microplate reader (DG5035, Huadong Electronics, Nanjing, Jiangsu, China).

To assess cell apoptosis, a deoxynucleotidyl transferase-mediated dUTP nick-end labeling (TUNEL) Cell Apoptosis Detection Kit (Cat No. G1502, Servicebio, Wuhan, Hubei, China) was used at 48 h post-transfection. The 10% formalin-fixed cells were cultivated with Equilibration Buffer for 10 minutes. Then the cells were stained in TUNEL working solution at 37 ℃ for 1 h. Next, DAPI (Cat No. G1012, Servicebio, Wuhan, Hubei, China) was incubated with the cells for 5 minutes. The cells were viewed under an inverted fluorescence microscope (AE31, Motic, Xiamen, Fujian, China).

For the Transwell assay, the cells were resuspended in FBS-free medium at 48 h post-transfection. The transwell inserts were coated with Matrigel Matrix (Cat No.356234, Corning, NY, USA) at 37 ℃ for 1 h. The cells were added to the transwell inserts, and the plate was filled with medium supplemented with 10% FBS. After 24 h of culture, the cells were fixed in 10% formalin. After the uninvaded cells were removed, the insert was stained in Crystal Violet Solution (Cat No. G1014, Servicebio, Wuhan, Hubei, China) for 15 minutes. Afterwards, the invaded cells were counted under the inverted microscope.

2.7 Chemosensitivity

Carboplatin (Cat No. HY-17393, MedChemExpress, Monmouth Junction, NJ, USA) was dissolved in culture medium with a range of concentrations (0, 10, 20, 40, 80 and 160 µg/mL). The SKOV3 and CAOV-3 cells were seeded in 96-well plates at 48 h after transfection. Then carboplatin-containing medium was cultivated the cells for 24 h. Next, the cells were cultured with CCK-8 reagent as described above. The optical density was recorded and the half-maximal inhibitory concentration IC_{50} was calculated.

2.8 Xenograft Assay

SKOV3 cells were transduced with LIMCH1 overexpression lentivirus (oeLIMCH1) or NC lentivirus (oeNC) (Genechem, Shanghai, China). After 72 h, stable transfectants were selected using 2 µg/mL puromycin for 7 days. Female BALB/c nude mice (4–6 weeks, 16–18 g, SLAC, Shanghai, China) were randomly divided into two groups

(n = 5 per group) and subcutaneously injected with 5×10^6 cells (oeNC or oeLIMCH1) in 100 µL PBS into the right axilla. Tumor volumes were measured weekly and calculated with a formula: $V = a \times b^2/2$, where a was the tumor length and b was the tumor width. After 4 weeks, mice were euthanized by cervical dislocation, and tumors were excised and weighed. All mice were housed in a specific-pathogen-free-grade animal facility at 25 °C with light/dark cycle of 12 h, and had free access to food and water. All animal procedures were approved by the Experimental Animal Welfare Ethics Committee of Nanjing Medical University (approval date: May 18, 2025). The assay was performed during the period from September 2025 to January 2026. The sample size was chosen based on the standard sample size commonly used in similar studies. All mice were grouped using random number table. Humane endpoints were predefined as tumor diameter exceeding 20 mm, severe ulceration, or >20% body weight loss. No mice reached these endpoints during the study.

2.9 Statistical Analysis

The data analysis and graph plotting were performed by GraphPad Prism 10 (GraphPad Software, Boston, MA, USA). Normality was assessed by Shapiro-Wilk test, and homogeneity of variances was verified by Bartlett's test. Differences among groups were compared using one-way analysis of variance (ANOVA), followed by Tukey's multiple comparisons test. The difference between the two groups was compared using the *t*-test or Mann–Whitney U test. The correlation was analyzed using Spearman correlation. The ability of LIMCH1 expression to predict ovarian cancer risk was analyzed using the receiver operating characteristic (ROC) curve. $p < 0.05$ was considered statistically significant.

3. Results

3.1 Candidate Genes Related to Ovarian Cancer Risk and Platinum Resistance

A total of 16,323 upregulated and 4500 downregulated DEGs from the GSE102094 dataset (Fig. 1A), 3103 upregulated and 5351 downregulated DEGs from the GSE160626 dataset (Fig. 1B), and 1178 upregulated and 3082 downregulated DEGs from the GSE190688 dataset (Fig. 1C) were identified in ovarian cancer tissues versus control tissues. Using intersection analysis, a total of 867 DEGs were identified as dysregulated across all three datasets (Fig. 1D), indicating they were highly correlated with ovarian cancer risk.

A total of 702 upregulated and 1023 downregulated DEGs from GSE102094 (Fig. 2A) and 123 upregulated and 4590 downregulated DEGs from the GSE160626 dataset (Fig. 2B) were identified in platinum-resistant versus platinum-sensitive ovarian cancer tissues, and were considered platinum-resistant DEGs. After intersecting the analysis of platinum-resistant DEGs in each dataset with the 867 DEGs highly correlated with ovarian cancer risk, 177 DEGs (57 + 12 + 108) were identified (Fig. 2C). They were considered candidate genes for ovarian cancer risk and platinum resistance, as listed in Table 1.

Subsequent enrichment analyses were carried out based on the 177 DEGs, which revealed that they were mainly enriched in biological processes related to cell cycle regulation, cell junctions, and neurogenesis (Fig. 3A), and were predominantly enriched in pathways related to carcinogenesis, cancer signaling, infections, and metabolism (Fig. 3B).

3.2 Validation of LIMCH1 and SNAI3 Expressions via Public Database and Clinical Sample Detection

Among the 177 candidate genes, LIMCH1 and SNAI3 were selected for further validation because both genes were consistently downregulated in ovarian cancer and platinum-resistant samples across datasets. In addition, a literature review indicated that the biological roles of LIMCH1 and SNAI3 in ovarian cancer remain largely unexplored, despite evidence suggesting potential tumor-suppressive functions in other malignancies. Therefore, these two genes were considered promising and novel candidates for further investigation.

Analysis of the GEPIA public database indicates that LIMCH1 expression was lower in ovarian cancer tissues than in control tissues (Fig. 4A). However, it was not significantly different among ovarian cancer patients with different tumor stages (Fig. 4B). Interestingly, extremely low expression of LIMCH1 was correlated with worse survival in ovarian cancer patients (Fig. 4C).

A cohort of 70 ovarian cancer patients was enrolled, with their clinical characteristics shown in Table 2. LIMCH1 expression was lower in tumor tissues than in control tissues (Fig. 4D,E). A further ROC curve revealed that LIMCH1 showed a strong ability to distinguish ovarian cancer from the control (AUC = 0.794, 95% CI: 0.650–0.938) (Fig. 4F). Importantly, LIMCH1 expression levels were negatively correlated with the International Federation of Gynecology and Obstetrics (FIGO) stage (Fig. 4G) and were also negatively associated with pathological grade in ovarian cancer patients (Fig. 4H).

SNAI3 expression did not differ between ovarian cancer tissues and control tissues and was not correlated with tumor stage and survival in ovarian cancer patients, as indicated by the GEPIA public database analysis (**Supplementary Fig. 1A–C**). Moreover, validation in ovarian cancer samples showed that its expression did not differ between tumor and control tissues (**Supplementary Fig. 1D,E**).

3.3 Effect of LIMCH1 on Ovarian Cancer Cells

Given the aforementioned clinical implications of LIMCH1 in ovarian cancer, it was selected for subsequent cellular experiments to validate its regulatory function.

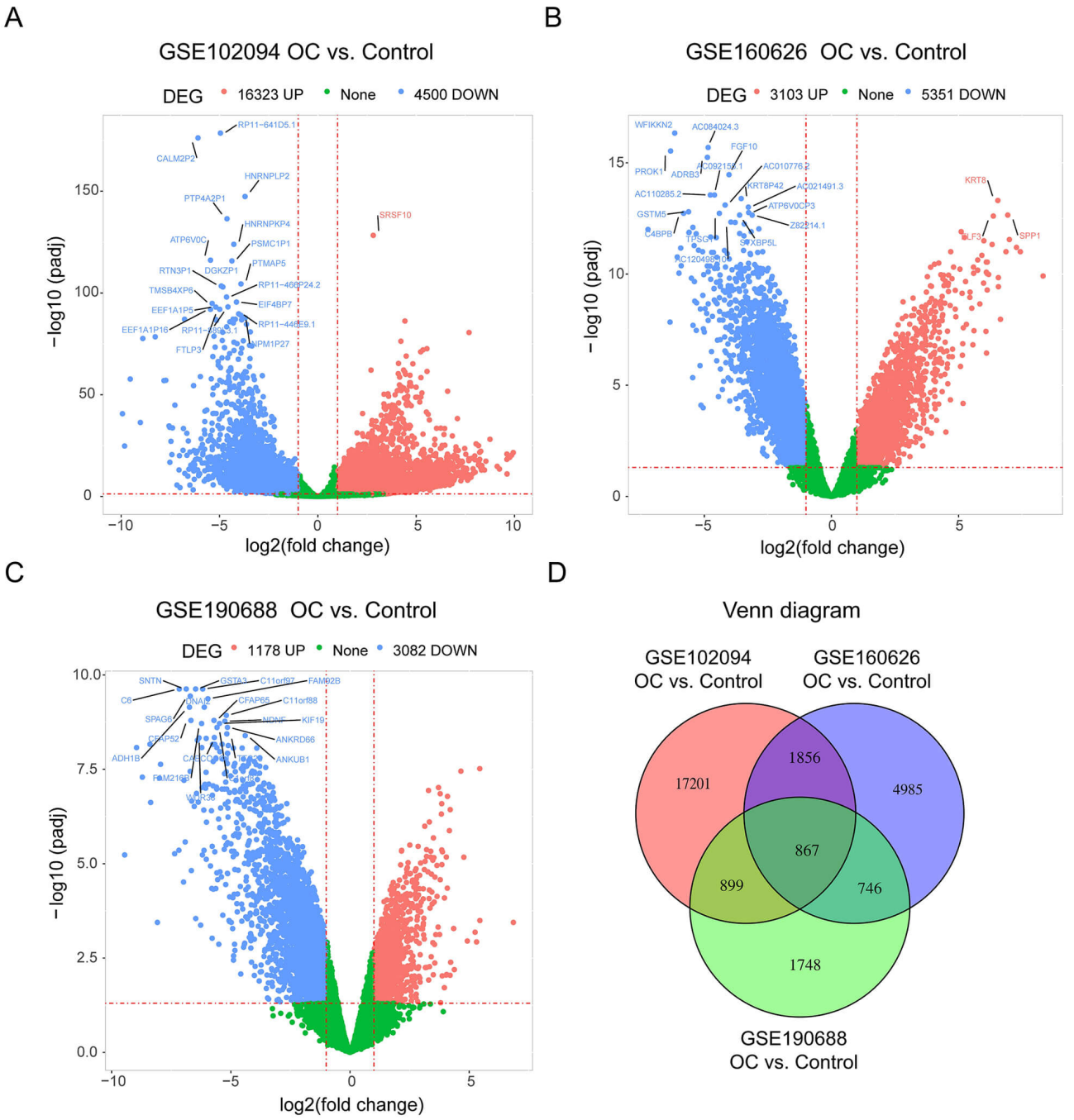

Fig. 1. DEGs in ovarian cancer tissues. DEGs in ovarian cancer tissues versus control tissues from GEO datasets: GSE102094 (A), GSE160626 (B), and GSE190688 (C). Intersecting analysis of the three datasets via a Venn diagram (D). DEGs, differentially expressed genes; OC, ovarian cancer.

LIMCH1 expression was elevated after transfection with LIMCH1 overexpression plasmids and reduced after transfection with LIMCH1 siRNA, suggesting successful transfection in SKOV3 cells (Fig. 5A,B). Cell proliferation and invasion were lower, while the apoptosis rate was higher after transfection with LIMCH1 overexpression plasmids in SKOV3 cells; by contrast, transfection with LIMCH1 siRNA showed the opposite effects (Fig. 5C–E). In CAOV-3 cells, the LIMCH1 expression, cell proliferation, invasion rate, and apoptosis rate showed the similar trend with those in SKOV3 cells after the transfection of LIMCH1 overexpression plasmids and LIMCH1 siRNA (**Supplementary Fig. 2A–E**).

3.4 Effect of LIMCH1 on Carboplatin Sensitivity in Ovarian Cancer Cells

In SKOV3 cells, the relative cell viability reduced with increasing carboplatin concentration (**Supplementary**

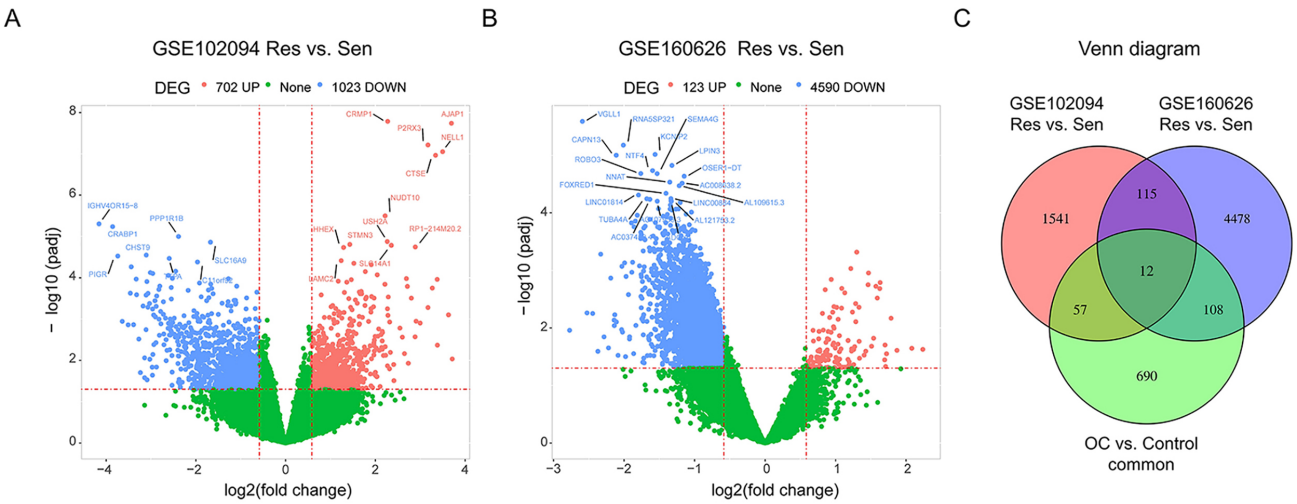

Fig. 2. DEGs in platinum-resistant ovarian cancer tissues. DEGs in platinum-resistant versus platinum-sensitive ovarian cancer tissues from GEO datasets: GSE102094 (A) and GSE160626 (B). Intersecting analysis using platinum-resistant DEGs in each dataset and the 867 DEGs that are highly correlated with ovarian cancer risk (C).

Table 1. List of candidate genes related to ovarian cancer risk and platinum resistance.

Gene symbol					
ACTA2-AS1	ADAMTS14	ADCY9	ADM2	ADRA2C	AIF1L
AK7	ALDH3B1	ALG3	AMIGO2	AMY1A	AMY1B
ANGPTL1	ARHGAP40	ARHGEF33	ARRB1	ASPG	BBS9
BCL2	C4BPA	C6orf223	CAPN13	CBX7	CCDC153
CCDC180	CCNF	CD40	CDC7	CDKL1	CENPW
CFB	CHEK1	CHST4	CIT	CORO2B	CRABP2
CST6	CXCL17	DAPK1	DMD	DNMBP	DNMT3B
DYDC2	E2F1	EBP	ESPL1	FAM111B	FAM13A
FAM153A	FAM181B	FAM83D	FAXDC2	FDXR	FEN1
FGF18	FHL1	FOXM1	FYCO1	GABRB3	GINS1
GJB2	GPR19	GRB14	GSDMC	GTSE1	GUCY1B2
HAND2	HAND2-AS1	HDAC5	HERC3	IGF2BP3	IGFBP6
IGSF23	IL20RB	IQGAP3	ISG15	JAM3	KCNMB3
KIF18B	KIF20A	KLHL13	KLK13	KLK5	KNTC1
KRT7	KRT86	KSR1	LAMC2	**LIMCH1**	LINC00839
LPAR3	LRFN5	LRGUK	LRP11	LRRC17	LRRN4CL
LTBP4	MAOB	MAPRE3	MCC	MEG3	MEIS2
MKI67	MMP7	MROH1	MROH6	MRPL12	MT1G
MYBL2	MYBPH	MYCL	NKAPP1	NMU	NUP210
NXPH4	OASL	OGDHL	PI3	PKHD1L1	PKP3
PLAU	PLCB1	PLCL1	PODN	PPFIA4	PPP1R3C
PRKCI	PSME2	PTPRN2	RAB3IL1	RAD54L	RASAL1
RASD1	RBM20	RFC4	RORC	RPS6KA6	S100A2
S100A7	SAMD10	SEMA6A	SFXN3	SHANK2	SLC35F2
SLC4A3	SLC9A3R1	SMIM5	**SNAI3**	SNCAIP	SNX33
SPAG17	SPATA6L	SSBP2	STXBP1	SYT13	TBC1D2B
TCF7	TEF	TGM1	THRA	TMEM255A	TPI1
TROAP	TSPAN5	TTC34	TTLL11	UBE2C	UBXN10
VEGFA	WDR49	XDH	XRCC2	ZC4H2	ZCCHC24
ZFPM2	ZNF462	ZNF609			

The bold font represented the genes selected for further validation.

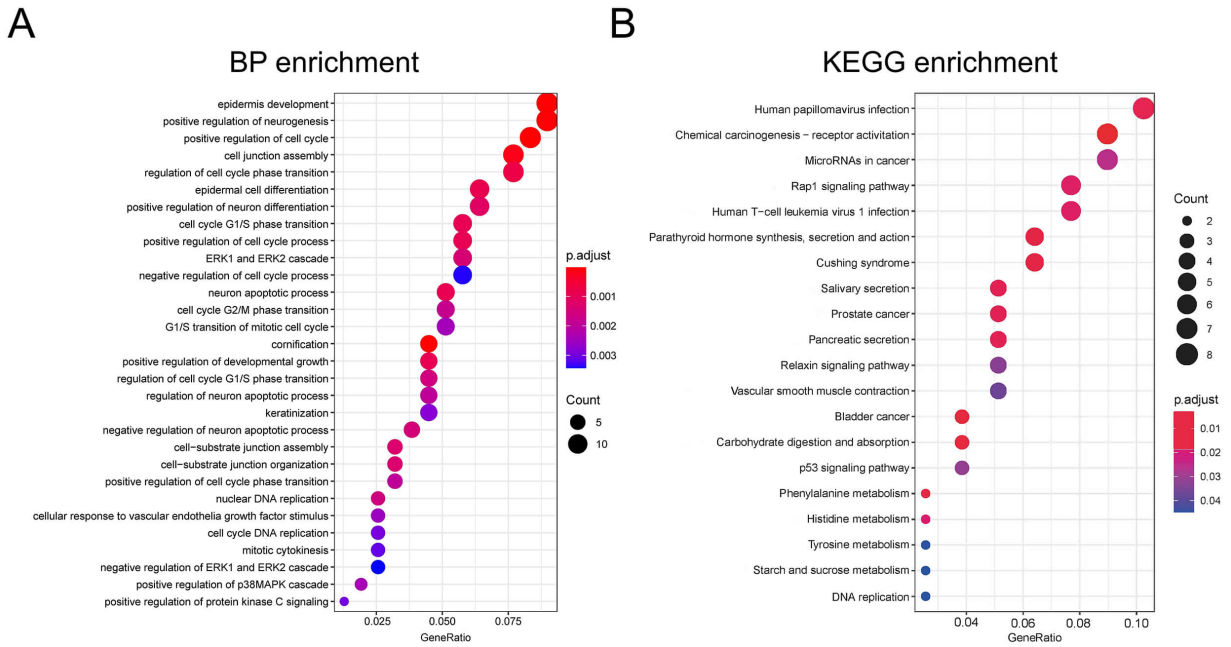

Fig. 3. Enrichment analysis. GO biological process enrichment (A) and KEGG pathway enrichment (B) analyses based on the 177 candidate DEGs. GO, Gene Ontology; KEGG, Kyoto Encyclopedia of Genes and Genomes.

Table 2. Characteristics of ovarian cancer patients.

Characteristics	Ovarian cancer patients (N = 70)
Age (years), mean ± SD	52.85 ± 10.50
FIGO stage, n (%)	
I	28 (40)
II	17 (24.3)
III	25 (35.7)
Pathological grade, n (%)	
G1	20 (28.6)
G2	12 (17.1)
G3	38 (54.3)
ECOG performance score, n (%)	
0	36 (51.4)
1	34 (48.6)
Subtype, n (%)	
High grade serous carcinoma	35 (50.0)
Low grade serous carcinoma	4 (5.7)
Endometrioid carcinoma	6 (8.6)
Clear cell carcinoma	16 (22.9)
Mucinous carcinoma	5 (7.1)
Others	4 (5.7)

SD, standard deviation; ECOG, Eastern Cooperative Oncology Group.

Fig. 3A). Furthermore, the IC_{50} decreased after transfection with LIMCH1 overexpression plasmid; by contrast, transfection with LIMCH1 siRNA showed the opposite effects (**Supplementary Fig. 3A**). In the CAOV-3 cells, relative cell viability and IC_{50} showed the similar trend with those in SKOV3 cells after transfection of LIMCH1 overexpression plasmids and LIMCH1 siRNA (**Supplementary Fig. 3B**).

3.5 Effect of LIMCH1 on Tumor Progression in Ovarian Cancer Mice

The tumor volume decreased after the transduction with LIMCH1 overexpression lentivirus (**Supplementary Fig. 4A**). Furthermore, the tumor weight also reduced after the transduction with LIMCH1 overexpression lentivirus (**Supplementary Fig. 4B**).

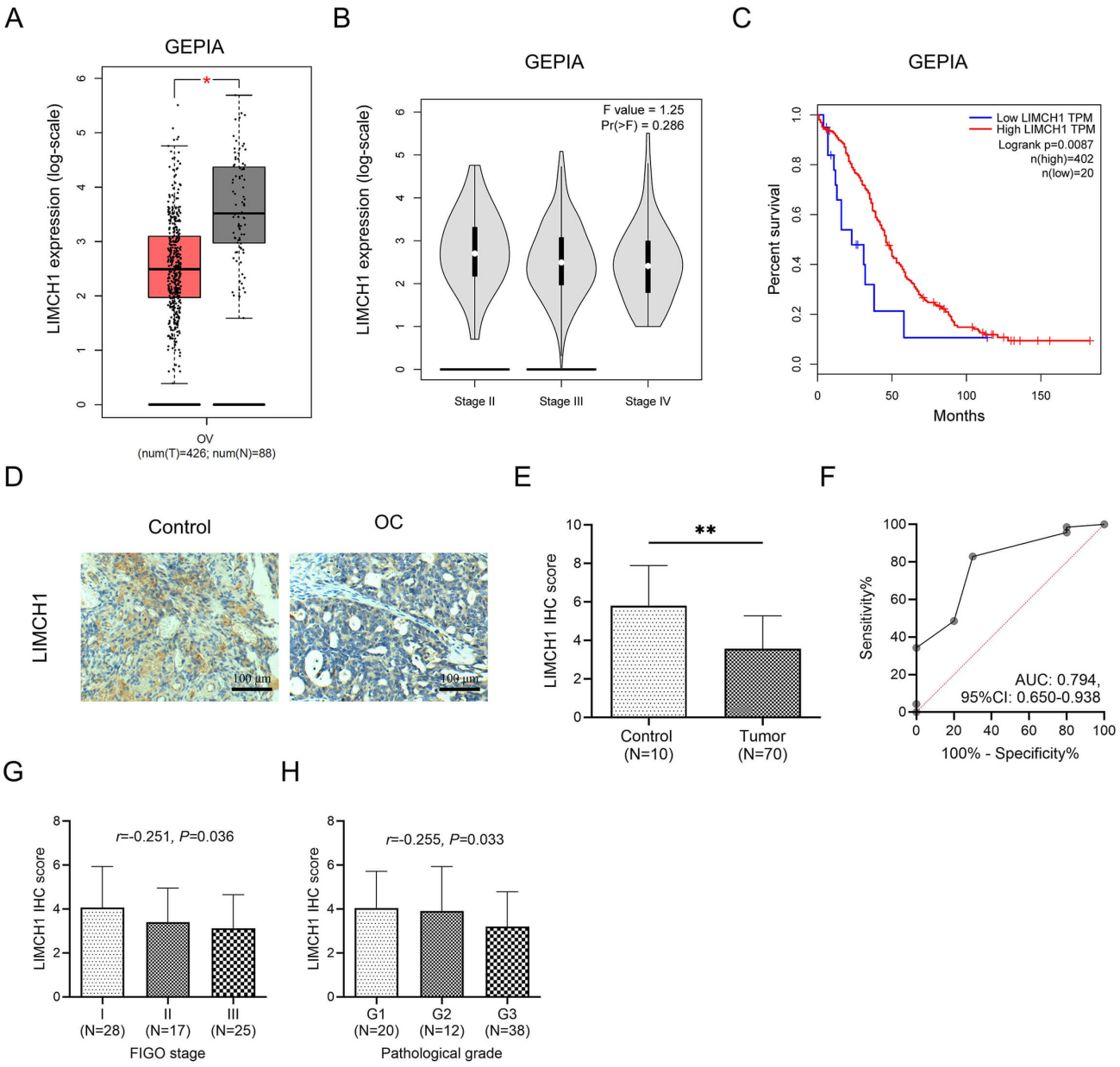

Fig. 4. Clinical relevance of LIMCH1 in ovarian cancer. Comparison of LIMCH1 expression between ovarian cancer tissues and control tissues (A), correlation of LIMCH1 expression with tumor stage in ovarian cancer patients (B), correlation of extremely low LIMCH1 expression with survival in ovarian cancer patients (C), via the analysis of the GEPIA public database. Validation of LIMCH1 expression between ovarian cancer tissues and control tissues via IHC staining (D) and quantitatively scoring (E) (analyzed by Mann–Whitney U test), ROC curve analysis of LIMCH1 expression in differentiating ovarian cancer from control (F), correlation of LIMCH1 expression with FIGO stage (G) and pathological grade (H) by Spearman correlation test in ovarian cancer patients, using clinical sample detections. LIMCH1, LIM and calponin homology domain-containing protein 1; GEPIA, Gene Expression Profiling Interactive Analysis; IHC, immunohistochemistry; ROC, receiver operating characteristic; FIGO, International Federation of Gynecology and Obstetrics. *p < 0.05; **p <0.01. Scale bar = 100 μm.

4. Discussion

In conjunction with advancements in high-throughput technologies such as RNA sequencing and microarrays, the landscape of genes associated with ovarian cancer risk has been largely elucidated [18,19,20]. For example, previous studies have identified numerous DEGs in ovarian cancer. Using microarray data, one study reported 164 upregulated and 80 downregulated DEGs in ovarian cancer tissues compared with control tissues [18], while an RNA sequencing study identified 333 upregulated and 273 downregulated DEGs [19]. Furthermore, analysis of large ArrayExpress datasets identified 59 upregulated and 431 downregu-

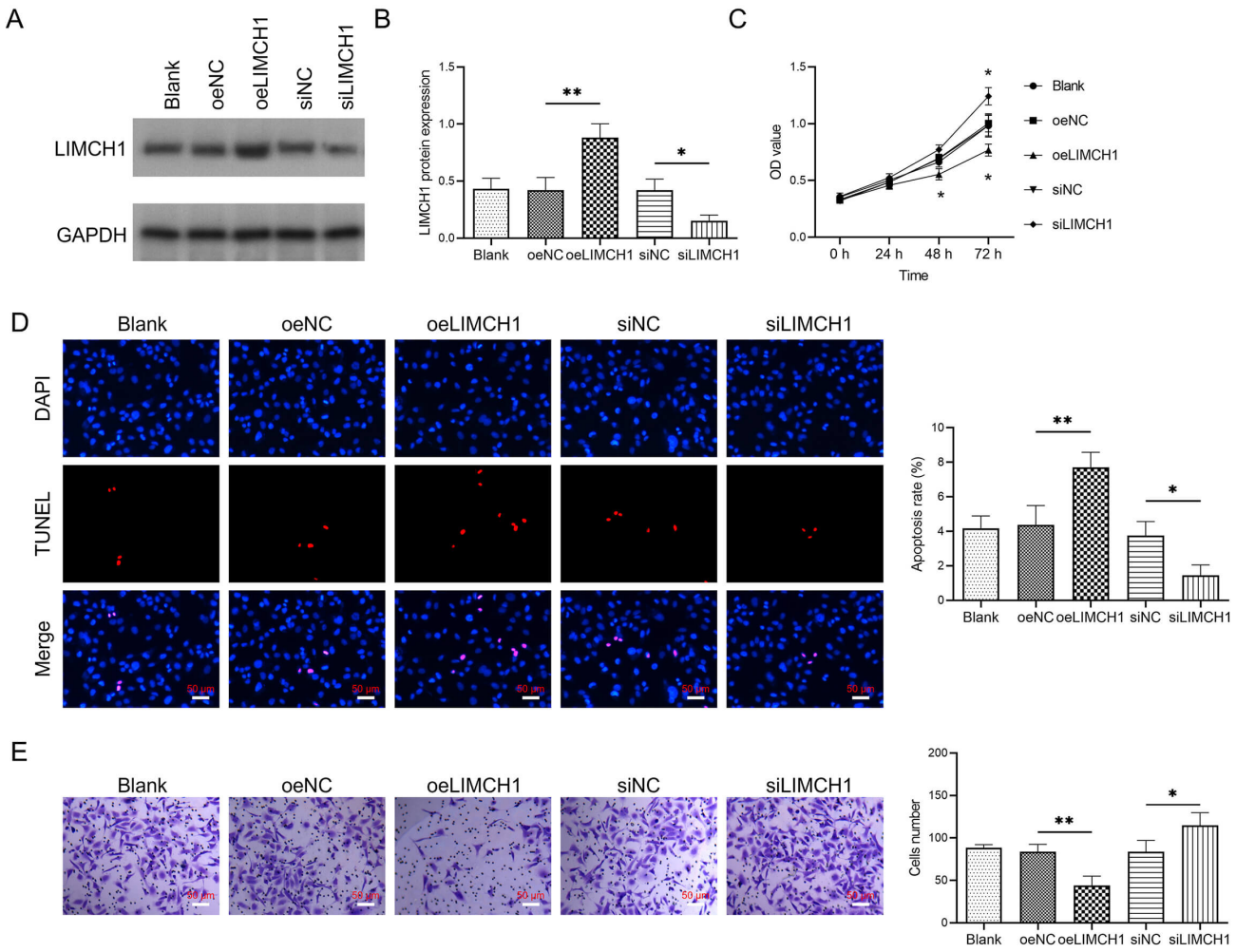

Fig. 5. Function of LIMCH1 in SKOV3 cells. Immunoblotting images (A) and quantitative expression of LIMCH1 (B) in SKOV3 cells after LIMCH1 overexpression plasmids and siRNA transfections. SKOV3 cell proliferation (C), apoptosis rate (D), and invasion (E) after LIMCH1 overexpression plasmids and siRNA transfections. Data were presented as mean ± standard deviation (SD) from three independent experiments (n = 3). Differences among groups were compared using one-way ANOVA, followed by Tukey's multiple comparisons test. ANOVA, analysis of variance. *$p < 0.05$, **$p < 0.01$. Scale bar = 50 μm.

lated DEGs in ovarian cancer tissues compared with controls [20]. Nevertheless, platinum-resistant ovarian cancer, as a more aggressive variant of ovarian malignancy, presents a significant concern that warrants further investigation [21]. Furthermore, there exists a scarcity of studies examining differentially expressed genes (DEGs) associated with both ovarian cancer susceptibility and platinum resistance. A total of 867 DEGs in ovarian cancer tissues compared with control tissues were identified by intersecting three GEO datasets, then cross-analyzed with DEGs in platinum-resistant versus platinum-sensitive ovarian cancer tissues from two GEO datasets, ultimately identifying 177 DEGs. In addition, the 177 DEGs were particularly enriched in biological processes related to cell cycle regulation and cell junctions via GO enrichment analysis, and in pathways related to carcinogenesis and cancer signaling via KEGG enrichment analysis. These findings suggest that the 177 DEGs may serve as candidate genes associated with ovarian cancer risk and platinum resistance through the regulation of cell cycle, cell junctions, and carcinogenesis signaling.

LIMCH1, a LIM and calponin homology domain protein, is widely expressed in human tissues, including the lungs, spleen, and ovary (https://www.bgee.org/gene/ENSG00000064042). Functionally, LIMCH1 acts as a myosin stress fiber-related protein, which can activate non-muscle myosin IIa, thereby positively regulating myosin stress fiber assembly and negatively regulating cell movement [22]. Additionally, LIMCH1 is considered a specific protein that regulates cell adhesion and actin cytoskeletal organization [23].

Recently, attention to the role of LIMCH1 as a tumor suppressor has been increasing [24,25,26]. A previous study reported that LIMCH1 was expressed at low levels in oral squamous cell carcinoma tissues compared with control tissues, and that its low expression was associated with

an increased risk of lymph node metastasis and poorer survival in patients with oral squamous cell carcinoma [24]. The other three relevant studies found that LIMCH1 was downregulated in lung cancer tissues and cell lines and was negatively correlated with tumor size, pleural invasion, and clinical stage in lung cancer patients, with high expression predicting a better prognosis [25,26,27]. Interestingly, a previous study used publicly available datasets for secondary bioinformatics analysis and found that LIMCH1 performed well at differentiating patients with serous ovarian cancer from healthy subjects [28]. Platinum-resistant ovarian cancer still lacks reliable biomarkers for clinical evaluation and prognosis prediction. Although several potential markers have been reported, their clinical applicability remains limited. LIMCH1 may therefore provide additional value for disease stratification and may be helpful in understanding tumor progression in ovarian cancer. The present study found that LIMCH1 was downregulated in ovarian cancer tissues versus control tissues, and its extremely low expression was correlated with worse survival in ovarian cancer patients via GEPIA public database analysis; afterward, via clinical sample verification, LIMCH1 was discovered to be lowly expressed in ovarian cancer tissues versus control tissues, and negatively correlated with tumor stage and grade in ovarian cancer patients. These findings are consistent with previous studies in other cancers [24,25,26,27], revealing the anti-tumor potency of LIMCH1 in ovarian cancer, which may be explained by its role in modulating myosin stress fibers and cell motility [22,23].

LIMCH1 is reported to repress tumor proliferation and migration while inducing tumor apoptosis in oral squamous cell carcinoma cells [24], and to suppress tumor growth via HUWE1-mediated P53 stability in lung cancer [25]. Moreover, LIMCH1 silencing promotes cell invasion in breast cancer [29]. To further validate the impact of LIMCH1 on ovarian cancer, cell-based experiments were performed, revealing that LIMCH1 decreased cell proliferation and invasion but increased apoptosis in ovarian cancer cells, thereby further validating its anti-tumor potency in ovarian cancer. This finding may be explained by its regulation of myosin stress fibers and cell motility [22,23], as well as its modulation of oncogenic pathways, such as P53 signaling [25].

Limitations

Some limitations in this study should be noted: (1) The cohort for validation of LIMCH1 expression was from a single center with a small sample size, which should be validated in a larger-sample-size study. (2) The SNAI3 was also chosen as the candidate gene for validation, while its expression was evaluated in only a limited number of clinical samples in the present study. Therefore, the potential diagnostic or prognostic value of a combined biomarker panel incorporating LIMCH1 and SNAI3 could not be comprehensively assessed. Futher study should be carried out for the validation. (3) The candidate genes in our study, including the LIMCH1 and SNAI3, were obtained from the public GEO database; however, heterogeneity and data processing pipelines might exist in these public databases. Therefore, further study by including the sample from our hospital and performing the transcriptomic analysis is needed. (4) The detailed mechanism of LIMCH1 in regulating the tumor progression and carboplatin sensitivity was not assessed in our study, which should be explored in further studies.

5. Conclusions

LIMCH1 is downregulated, and its low expression correlates with poor prognosis in ovarian cancer patients. Additionally, LIMCH1 suppresses ovarian cancer cell growth and invasion. These findings indicate the potential tumor-suppressive role of LIMCH1 in ovarian cancer. Nonetheless, additional validation studies are required to confirm these findings.

Abbreviations

LIMCH1, LIM and calponin homology domain-containing protein 1; DEGs, differentially expressed genes; GEPIA, Gene Expression Profiling Interactive Analysis; VEGF, vascular endothelial growth factor; GEO, Gene Expression Omnibus; GO, Gene Ontology; KEGG, Kyoto Encyclopedia of Genes and Genomes; SNAI3, Snail family transcriptional repressor 3; IHC, immunohistochemistry; ANOVA, analysis of variance; ROC, receiver operating characteristic.

Availability of Data and Materials

The datasets (GSE102094, GSE160626, and GSE190688) used or analyzed during the current study are available from the corresponding author on reasonable request.

Author Contributions

PZ: Conceptualization, formal analysis, methodology, project administration, writing - original draft, writing - review & editing; XF, YW, JY: Data curation, investigation, resources, writing - original draft, writing - review & editing; YC: Conceptualization, formal analysis, methodology, supervision, writing - original draft, writing - review & editing. All authors contributed to editorial changes in the manuscript. All authors read and approved the final manuscript. All authors have participated sufficiently in the work and agreed to be accountable for all aspects of the work.

Ethics Approval and Consent to Participate

This study was approved by the Medical Ethics Committee of Changzhou Maternal and Child Health Care Hospital (approval No. 2023 [156], approval date: October 11, 2023). All patients or their families provided written in-

formed consent. The study was conducted in accordance with the Declaration of Helsinki. The animal experiments were approved by the Experimental Animal Welfare Ethics Committee of Nanjing Medical University (approval date: May 18, 2025). And the animal experiments were performed in accordance with the Animal Research: Reporting of In Vivo Experiments (ARRIVE) guidelines, the principles of Replacement, Reduction, and Refinement (3Rs), as well as institutional and national guidelines for the care and use of laboratory animals.

Acknowledgment

Not applicable.

Funding

This study was supported by the Changzhou Municipal Health Commission's Leading Project (Research on Clinical Frontier Technologies) (No. WJJBGS202505), the Application Foundation Project of Changzhou Science and Technology Bureau (No. CJ20245041), the Science and Technology Development Foundation Project of Nanjing Medical University (No. NMUB20240054), the Science and Technology Development Foundation Project of Nanjing Medical University (No. NMUB20230054), and the Research project of Changzhou Maternal and Child Health Hospital (No. YJ202408).

Conflicts of Interest

The authors declare no conflicts of interest.

Supplementary Material

Supplementary material associated with this article can be found in the online version at https://doi.org/10.31083/CEOG52944.

References

[1] Bray F, Laversanne M, Sung H, Ferlay J, Siegel RL, Soerjomataram I, et al. Global cancer statistics 2022: GLOBOCAN estimates of incidence and mortality worldwide for 36 cancers in 185 countries. CA: a Cancer Journal for Clinicians. 2024; 74: 229–263. https://doi.org/10.3322/caac.21834

[2] Han B, Zheng R, Zeng H, Wang S, Sun K, Chen R, et al. Cancer incidence and mortality in China, 2022. Journal of the National Cancer Center. 2024; 4: 47–53. https://doi.org/10.1016/j.jncc.2024.01.006

[3] Nag S, Ray Coquard I, Gupta S, Pathak A, Li N, Mulya Sari R, et al. Pan-Asia adapted ESMO Clinical Practice Guideline for the management of patients with newly diagnosed and relapsed epithelial ovarian cancer. ESMO Open. 2025; 10: 105125. https://doi.org/10.1016/j.esmoop.2025.105125

[4] Di Berardino S, Bizzarri N, Ciancia M, Moro F, Padial Urtueta B, Marchetti C, et al. Value of frozen section to tailor surgical staging in apparent early-stage epithelial ovarian cancer. International Journal of Gynecological Cancer : Official Journal of the International Gynecological Cancer Society. 2025; 35: 101746. https://doi.org/10.1016/j.ijgc.2025.101746

[5] Rai L, Ravaggi A, Bignotti E, Hollis RL, Garsed DW, Pandey A, et al. Oxford Classic-Defined EMT Risk Stratification of High-Grade Serous Ovarian Cancer for Guiding Treatment Decisions. Clinical Cancer Research : an Official Journal of the American Association for Cancer Research. 2026; 32: 188–202. https://doi.org/10.1158/1078-0432.CCR-24-4250

[6] Caruso G, Weroha SJ, Cliby W. Ovarian Cancer: A Review. JAMA. 2025; 334: 1278–1291. https://doi.org/10.1001/jama.2025.9495

[7] Tropé C, Kaern J. Adjuvant chemotherapy for early-stage ovarian cancer: review of the literature. Journal of Clinical Oncology : Official Journal of the American Society of Clinical Oncology. 2007; 25: 2909–2920. https://doi.org/10.1200/JCO.2007.11.1013

[8] Barretina-Ginesta MP, Redondo A, Cortés-Salgado A, Madariaga A, Pérez-Mies B, Sancho L, et al. Assessing platinum response in first-line advanced ovarian cancer: clinical implications and future directions. International Journal of Gynecological Cancer : Official Journal of the International Gynecological Cancer Society. 2026; 36: 104684. https://doi.org/10.1016/j.ijgc.2026.104684

[9] St Laurent J, Liu JF. Treatment Approaches for Platinum-Resistant Ovarian Cancer. Journal of Clinical Oncology : Official Journal of the American Society of Clinical Oncology. 2024; 42: 127–133. https://doi.org/10.1200/JCO.23.01771

[10] Wang CC, Gomez-Roas M, Hinchcliff EM. Emerging Therapeutic Targets for Platinum-Resistant Ovarian Cancer. Hematology/oncology Clinics of North America. 2025; 39: 1057–1075. https://doi.org/10.1016/j.hoc.2025.04.019

[11] Shah M, Chen TY, Ison G, Fiero MH, Zhang H, Gao X, et al. Overall Survival and the Evolving Benefit-Risk Assessment for Poly (ADP-ribose) Polymerase Inhibitors in Advanced Ovarian Cancer. Journal of Clinical Oncology : Official Journal of the American Society of Clinical Oncology. 2025; 43: 2218–2227. https://doi.org/10.1200/JCO-24-02834

[12] Gaitskell K, Rogozińska E, Platt S, Chen Y, Abd El Aziz M, Tattersall A, et al. Angiogenesis inhibitors for the treatment of epithelial ovarian cancer. The Cochrane Database of Systematic Reviews. 2023; 4: CD007930. https://doi.org/10.1002/14651858.CD007930.pub3

[13] Yang YF, Rui L, Zhang BW, Huang T, Shao GB. Autophagy regulation in ovarian cancer chemoresistance: Molecular mechanisms and emerging frontiers. Life Sciences. 2025; 380: 123966. https://doi.org/10.1016/j.lfs.2025.123966

[14] Nunes M, Bartosch C, Abreu MH, Richardson A, Almeida R, Ricardo S. Deciphering the Molecular Mechanisms behind Drug Resistance in Ovarian Cancer to Unlock Efficient Treatment Options. Cells. 2024; 13: 786. https://doi.org/10.3390/cells13090786

[15] Wang G, Yang H, Wang Y, Qin J. Ovarian cancer targeted therapy: current landscape and future challenges. Frontiers in Oncology. 2025; 15: 1535235. https://doi.org/10.3389/fonc.2025.1535235

[16] Yang J, Wang Y, Liu F, Zhang Y, Han F. Crosstalk between ferroptosis and endoplasmic reticulum stress: A potential target for ovarian cancer therapy (Review). International Journal of Molecular Medicine. 2025; 55: 97. https://doi.org/10.3892/ijmm.2025.5538

[17] Tang Z, Li C, Kang B, Gao G, Li C, Zhang Z. GEPIA: a web server for cancer and normal gene expression profiling and interactive analyses. Nucleic Acids Research. 2017; 45: W98–W102. https://doi.org/10.1093/nar/gkx247

[18] Tang W, Li J, Chang X, Jia L, Tang Q, Wang Y, et al. Construction of a novel prognostic-predicting model correlated to ovarian cancer. Bioscience Reports. 2020; 40: BSR20201261. https://doi.org/10.1042/BSR20201261

[19] Siavoshi A, Taghizadeh M, Dookhe E, Piran M. Gene expression profiles and pathway enrichment analysis to identification

of differentially expressed gene and signaling pathways in epithelial ovarian cancer based on high-throughput RNA-seq data. Genomics. 2022; 114: 161–170. https://doi.org/10.1016/j.ygeno.2021.11.031

[20] Lu X, Wang J, Shan X, Li Y. Selecting key genes associated with ovarian cancer based on differential expression network. Journal of B.U.ON. : Official Journal of the Balkan Union of Oncology. 2017; 22: 48–57.

[21] Lin H, Wu CH, Fu HC, Ou YC. Evolving treatment paradigms for platinum-resistant ovarian cancer: an update narrative review. Taiwanese Journal of Obstetrics and Gynecology. 2024; 63: 471–478. https://doi.org/10.1016/j.tjog.2024.05.006

[22] Lin YH, Zhen YY, Chien KY, Lee IC, Lin WC, Chen MY, et al. LIMCH1 regulates nonmuscle myosin-II activity and suppresses cell migration. Molecular Biology of the Cell. 2017; 28: 1054–1065. https://doi.org/10.1091/mbc.E15-04-0218

[23] Maddala R, Eldawy C, Bachman W, Soderblom EJ, Rao PV. Glypican-4 regulated actin cytoskeletal reorganization in glucocorticoid treated trabecular meshwork cells and involvement of Wnt/PCP signaling. Journal of Cellular Physiology. 2023; 238: 631–646. https://doi.org/10.1002/jcp.30953

[24] Xu L, Shi W, Li Y, Shen Y, Xie S, Shan X, et al. LIM and calponin homology domains 1 may function as promising biological markers to aid in the prognostic prediction of oral squamous cell carcinoma. Beijing Da Xue Xue Bao. Yi Xue Ban = Journal of Peking University. Health Sciences. 2025; 57: 19–25. https://doi.org/10.19723/j.issn.1671-167X.2025.01.004

[25] Zhang Y, Zhang Y, Xu H. LIMCH1 suppress the growth of lung cancer by interacting with HUWE1 to sustain p53 stability. Gene. 2019; 712: 143963. https://doi.org/10.1016/j.gene.2019.143963

[26] Cao H, Zhao J, Chen Z, Sun W, Ruan K, Zhou J, et al. Loss of LIMCH1 predicts poor prognosis in patients with surgically resected Lung Adenocarcinoma: A study based on Immunohistochemical Analysis and Bioinformatics. Journal of Cancer. 2021; 12: 181–189. https://doi.org/10.7150/jca.47883

[27] Karlsson T, Kvarnbrink S, Holmlund C, Botling J, Micke P, Henriksson R, et al. LMO7 and LIMCH1 interact with LRIG proteins in lung cancer, with prognostic implications for early-stage disease. Lung Cancer (Amsterdam, Netherlands). 2018; 125: 174–184. https://doi.org/10.1016/j.lungcan.2018.09.017

[28] Kasavi C. Gene co-expression network analysis revealed novel biomarkers for ovarian cancer. Frontiers in Genetics. 2022; 13: 971845. https://doi.org/10.3389/fgene.2022.971845

[29] Bersini S, Lytle NK, Schulte R, Huang L, Wahl GM, Hetzer MW. Nup93 regulates breast tumor growth by modulating cell proliferation and actin cytoskeleton remodeling. Life Science Alliance. 2020; 3: e201900623. https://doi.org/10.26508/lsa.201900623